QUANTITATIVE EVALUATION STUDY OF BUS OUTER PANEL SURFACE DAMAGE BASED ON 3D MORPHOLOGICAL ANALYSIS

Xing WANG[1,*], Mingming WU[2], Yan LIU[3], Xiaochun ZHANG[4]

This study utilizes a stamping machine, laser cutter, and three-dimensional texture analyzer to quantitatively evaluate surface damage during the stamping process. The evaluation parameters are S_q, S_{sk}, S_{ku}, and S_{pd}. Through MATLAB simulation software and orthogonal experimental optimization analysis, more precise parameter thresholds are obtained: S_q = 4.84 μm, S_{sk} = -0.026 μm, S_{ku} = 3.57 μm, and S_{pd} = 167mm^{-2}. The test results show that surface three-dimensional roughness measurement can distinguish different morphological features of stamping parts' surfaces and describe their features.

Keywords: 3D surface roughness; Surface damage; Morphological characteristics; Orthogonal experiment; MATLAB.

1. Introduction

Surface damage during stamping is the result of relative sliding friction between the sheet metal and the surface of the die, which reduces the collision safety, corrosion resistance, fatigue resistance, and paint adhesion of the stamped parts, and can lead to part failure. In order to control surface damage during stamping, it is important to evaluate the surface roughness of stamped parts properly, measure its numerical value correctly, and study the relationship between evaluation parameters and functional characteristics of use in depth.

Currently, the two-dimensional evaluation standard of surface roughness for stamped parts has been widely used (iso4287:1997). However, the two-dimensional evaluation standard only evaluates a surface based on data from a single line, which cannot reflect the entire surface's micro-topography and characterization is relatively incomplete. With the advancement of technology and in-depth research on surface analysis, the 3D roughness evaluation of stamped parts can provide

[1] Prof., School of Robot Engineering, Anhui Sanlian University, China, e-mail: hfwangxing@gmail.com
[2] Prof., School of Automotive Engineering， Wuhu University， China， e-mail：wmm19842002@163.com
[3] Eng., Anhui BoWan Robotics Co., Ltd., China, e-mail: 1163485720@qq.com
[4] Assoc. Prof., School of Mechanical Engineering, Tongling Polytechnic, China, e-mail: 382075139@qq.com

complete information about the surface (iso25178:2012). It can fully reflect the actual measured surface and describe the surface morphology characteristics of the part as a whole, with a global perspective. Therefore, the trend in mechanical stamping processing quality development is to replace two-dimensional roughness characterization with 3D roughness characterization.

The origins of 3D surface morphology analysis can be traced back to the 1970s when Grieve et al. designed a simple operating system to record parallel contour lines and draw contour maps [1]. In the 1980s, the advent and popularization of personal computers made spatial analysis possible, which accelerated the development of 3D surface morphology analysis [2]. In the 1990s, Stout and Sullivan used Sa, Sq, Ssk, and Sku parameters to study the surface of rolled steel plates, demonstrating how to use 3D characterization technology to qualitatively and quantitatively analyze engineering surfaces [3]. Dong and Sullivan conducted comprehensive research on surface wear, defining and algorithmically calculating amplitude and some function parameters. They discussed the feasibility of sampling conditions and the applicability of parameters [4]. Xie and Chen measured the 3D surface morphology of several steel plates processed by different techniques, obtaining the two-dimensional power spectral density function, the two-dimensional autocorrelation function, and two 3D characteristic parameters for each surface morphology [5]. In just over 20 years of this century, the application of 3D surface roughness has become more widespread in manufacturing and materials. In 2003, Suh and Polycarpou studied the wear of discs and steel pins, conducting a detailed study of surface morphology using one- and two-dimensional analyses [6]. In 2004, Ramasawmy et al. studied the effects of different EDM parameters, such as discharge current, discharge time, and discharge interval, on surface roughness, surface morphology, and form errors of workpieces. The results of the study can help optimize the EDM process to achieve better surface quality and shape accuracy [7]. In 2011, Czifra and Horváth investigated the performance of sliding friction and analyzed the effects of surface morphology on the friction and wear between ground steel samples with different machining directions and different surface quality grades and sliding friction pairs [8]. In 2012, Ereifej et al. studied the effects of different polishing techniques on the three-dimensional surface roughness and gloss of dental restorative resin composites [9]. In 2014, Deltombe et al. introduced an experimental device and method for measuring the surface roughness of test samples, as well as how to apply different three-dimensional roughness parameters to the samples. The authors also discussed the advantages and limitations of different three-dimensional roughness parameters and how to choose the most relevant parameters for specific applications [10]. In 2014, Kumar et al. analyzed the evolution of surface morphology features and quantitative three-dimensional surface texture parameters. Using confocal laser scanning microscopy, the changes in average surface roughness deviation (Sa),

standard deviation of roughness (Sq), average roughness depth (Sz), and surface skewness (Ssk) with ablation timewere evaluated, as well as the corresponding two-dimensional line roughness parameters Ra, Rq, Rz, and Rsk, to determine the damage mechanism of steel [11]. In 2015, Hoła et al. studied the usefulness of three-dimensional surface roughness parameters for non-destructive evaluation of concrete layer tensile adhesion. The article describes an experimental device and method for measuring the tensile adhesion of concrete layers and how to use three-dimensional surface roughness parameters to analyze the surface morphology of test samples [12]. In 2015, Logins et al. studied the effects of different high-speed milling strategies on three-dimensional surface roughness parameters. The authors also discussed the relationship between milling parameters such as feed rate and spindle speed and three-dimensional surface roughness parameters, as well as how different milling strategies affect the three-dimensional surface roughness of the workpiece [13]. In 2016, Przestacki et al. used laser cladding technology to form a coating on the surface of stainless steel and studied the effects of different process parameters on the three-dimensional surface roughness and texture of the cladding layer to better control the three-dimensional surface roughness and achieve the desired surface characteristics [14]. In 2017, Lazoglu used five-axis ball head milling technology to machine some workpieces under different parameters and studied the relationship between different surface parameters such as Sa, Sq, and Sz, and proposed some conclusions and recommendations to better understand and apply thesesurface parameters [15]. In 2019, K. Maňas et al. measured and analyzed the texture of joint sample surfaces using 2D and 3D surface morphology analysis techniques, and studied the relationship between different surface parameters such as Ra, Rz, and Sa, and evaluated the effects of these surface parameters on the surface quality and performance of joint samples [16]. In 2021, Viktor Molnár introduced a new method for minimizing the evaluation area of three-dimensional surface roughness. The article describes the development of this method and its application in measuring the surface roughness of several different materials. The author also discussed the advantages of this new method over traditional methods and how it improves the accuracy and efficiency of three-dimensional surface roughness measurement [17]. In 2022, Thasana et al. used virtual machining technology to generate plastic injection parts with different surface roughness, and modeled and predicted the three-dimensional surface roughness parameters of the injection parts' gloss using artificial neural network technology [18].

With the passage of time and differences in research content, scholars from various countries mostly use three-dimensional surface roughness parameters to analyze the correlation between various material surface functions and three-dimensional surface characterization. However, there is relatively little research on surface quality analysis of metal stamping parts. The traditional angle of two-dimensional surface roughness parameters can often only qualitatively or semi-

quantitatively evaluate the quality of stamping parts, and rarely consider the performance of the parts in use from the perspective of production. Therefore, the significance of this study is to determine evaluation parameters based on the wear resistance performance that the material needs to have during the stamping process, measure the parameters at relevant positions using a profilometer, determine qualified samples according to on-site quality inspection standards, roughly calculate the threshold values of three-dimensional roughness parameters that affect surface quality through physical experiments, and further optimize and analyze the parameter threshold values through simulation experiments to obtain more accurate threshold values. This will help improve the quality and reliability of metal stamping parts and promote the development of stamping processing technology.

2. Plate material and experimental plan

DC56 steel plate is often used to make surface coverings for buses. The blank for the experiment is selected from 2mm thick plate material from Baoshan Iron & Steel Co., Ltd. in Shanghai, China. The main performance parameters of this type of steel plate are shown in Table 1.

Table 1

Main performance parameters of DC56 steel plate

Yield strength (MPa)	Tensile strength (MPa)	R-value	N-value	K value
156	297	2.3	0.235	530

The chemical composition of the plate material is mainly: C (carbon): ≤0.12 wt%, Si (silicon): ≤0.5 wt%, Mn (manganese): ≤0.6 wt%, P (phosphorus): ≤0.1 wt%, S (sulfur): ≤0.045 wt%, Ti (titanium): ≤0.3 wt%, Nb+Ti: ≤0.3 wt%.

The stamping molds in the production workshop include door, roof, side panel, lamp holder, etc. In order to reduce the number of experiments and the difficulty of testing, this study selected the rear lamp holder as the target part with typical shape features. The reason is that it undergoes large deformation during stamping and the local surface angles formed with the stamping direction can simulate different parts of the vehicle body.

2.1 Experimental procedure

The specimens used in the experiment were taken from different characteristic positions of the target stamped part, as shown in Fig 1. These positions included Z_1, Z_2, and Z_3, which simulated gentle surfaces; Y_1, Y_2, and Y_3, which simulated bent corners; Y_4 and Y_5, which simulated large-angle deep-drawn surfaces; and one randomly selected part from a production cycle as the research sample. When obtaining the specimens, the feature surface domains were first cut from the part using a 3D laser cutting machine to form specimens with a diameter

of 10mm, as shown in Fig 2. A total of 8 specimens were obtained and then cleaned with ultrasonic waves and dried with oil-free compressed air.

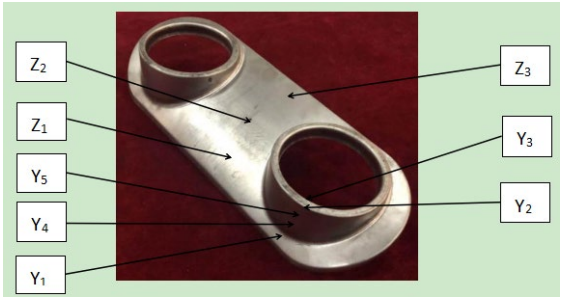

Fig. 1. Characteristic positions

Fig. 2. Obtaining specimens.

The profilometer used in this experiment is the TR-Scan-P non-contact surface micro-topography measuring instrument produced by TRIMOS, Switzerland. As shown in Fig 3, the system uses TRIMOS technology digital holographic microscopy (DHM) for 3D microscopic surface inspection with high precision. The instrument's control, testing, and data processing are all realized by computer systems and related software, with X and Y coordinates used for positioning and scanning of planar points, and the Z axis used for focusing and movement. Its greatest feature is the use of non-contact measurement principles for non-destructive detection of surface roughness and micro-topography.

Fig. 3. 3D profilometer

The TRIMOS TR-Scan-P 3D profilometer was used to pick up a 2mm × 2mm square measurement area at the center position of each of the 8 specimens, with a measurement step of 10μm and 3 measurements taken for each specimen to obtain the median value. The obtained measurement results were processed in the NanoWare surface analysis software. The original 3D surface morphology data $f_1(x,y)$ was corrected by the least squares method to obtain the corrected data morphology $f_2(x,y)$. The corrected data morphology was then subjected to

regression Gaussian filtering to obtain the 3D surface roughness evaluation benchmark w(x,y), and the 3D surface roughness morphology was obtained as $z(x,y)=f_2(x,y)-w(x,y)$. Based on ISO 25178:2012, parameters with significant correlation to friction and wear were selected, and the changes in related morphology parameters were statistically analyzed. At the same time, according to He Yuanfang's introduction of the surface quality classification and evaluation method for bus body covers [19], preliminary parameter thresholds were obtained from the qualified products inspected. Finally, the orthogonal experimental method was used to further optimize and analyze the parameter thresholds to obtain more accurate values.

2.2 Selection of Roughness Evaluation Parameters

To avoid the "parameter inflation" phenomenon similar to that in two-dimensional evaluations, the selection of 3D roughness parameters should be based on the principles of minimal, basic, and important choices to evaluate surface quality. In this study, four 3D parameters that can comprehensively evaluate the surface roughness of stamped parts were selected based on the IS025178:2012 parameter system and the characteristics of stamping-formed surfaces [20]. The mathematical expressions for these parameters are shown in Table 2.

Table 2

Selected 3D roughness evaluation parameters and their mathematical expressions

Parameter	Definition Expression	Discretization Mathematical Expression
S_q	$\sqrt{\frac{1}{A}\iint_A z^2(x,y)dxdy}$	$\sqrt{\frac{1}{mn}\sum_{i=1}^{m}\sum_{j=1}^{n} z^2(i,j)}$
S_{sk}	$\frac{1}{S_q^{\,3}}\left[\frac{1}{A}\iint_A z^3(x,y)dxdy\right]$	$\frac{1}{S_q^{\,3}}\left[\frac{1}{mn}\sum_{i=1}^{m}\sum_{j=1}^{n} z^3(i,j)\right]$
S_{ku}	$\frac{1}{S_q^{\,4}}\left[\frac{1}{A}\iint_A z^4(x,y)dxdy\right]$	$\frac{1}{S_q^{\,4}}\left[\frac{1}{mn}\sum_{i=1}^{m}\sum_{j=1}^{n} z^4(i,j)\right]$
S_{pd}	$S_{pd}=FC_{;}H_{;}\text{wolfprune}:\text{X}\%_{;}$ $ALL_{;}C\text{ount}_{;}D\text{ensity}_{;}$ Unless otherwise specified, X defaults to 5. Wolfprune represents a spatial filter; FC represents feature description; H represents small mountain structures in the sampling area.	——

(1) Root mean square deviation (S_q): This parameter represents the deviation of the contour from the reference plane. For stamped surfaces with strong randomness and many random points or structures, this parameter can more accurately reflect the height statistical characteristics of the stamped surface.

(2) Skewness (S_{sk}): Skewness is a parameter that measures the asymmetry of the amplitude distribution curve relative to the neutral plane. It is simple and practical and directly affects the friction and wear performance of the part surface.

(3) Kurtosis (S_{ku}): Kurtosis reflects the sharpness of the changes in the contour amplitude distribution curve. The smaller the value of the surface morphology steepness, the flatter and wider the height distribution curve, and vice versa. It is very effective in predicting the wear and lubrication-related performance of parts.

(4) Peak density (S_{pd}): Peak density represents the number of peaks in a unit sampling area. This parameter characterizes the spatial characteristics of the surface morphology and has a significant impact on the friction and wear performance of the surface. It is also particularly sensitive to noise.

2.3 Algorithm Principle

The 3D surface fast Gaussian filtering convolution algorithm [21] utilizes the iterative and separable properties of the two-dimensional Gaussian function, greatly reducing the number of exponential operations and improving the calculation speed. Therefore, this algorithm is used to obtain the 3D surface roughness evaluation benchmark. Based on regression Gaussian filtering, the 3D Gaussian benchmark surface for stamped parts is discretely defined as:

$$\begin{cases} w(i,j) = \dfrac{\sum\limits_{n=x_3}^{x_4}\left[\sum\limits_{m=x_1}^{x_2} z(i-m,j-n)g(m)\right]g(n)}{\sum\limits_{m=x_1}^{x_2} g(m)\sum\limits_{n=x_3}^{x_4} g(n)} \\ i = x_1,\cdots,x_2+m;\ j = x_3,\cdots,x_4+n \\ g(m) = \dfrac{1}{\alpha\lambda_{cx}}\exp\left[-\pi\left(\dfrac{m\Delta x}{\alpha\lambda_{cx}}\right)^2\right] \\ g(n) = \dfrac{1}{\alpha\lambda_{cy}}\exp\left[-\pi\left(\dfrac{n\Delta y}{\alpha\lambda_{cy}}\right)^2\right] \end{cases} \tag{1}$$

In the equation:

$z(i-m,j-n)$: Discrete representation of 3D contour sampling data

$w(i,j)$: Discrete form of Gaussian reference plane

$g(m), g(n)$: Regression Gaussian filtering weight function

m and n: number of points in the x and y directions of the sampled data

x_1, x_2, x_3, x_4: Range of calibrated Gaussian density function and weighted average

Δx and Δy: Sampling intervals in the x and y directions

When the pass rate of the Gaussian density function is 0.5, α is set to 0.4697.

3. Experimental Results and Analysis

3.1 Selection of Samples with Qualified Surface Quality

Based on He Yuanfang's classification of surface quality standards for bus exterior parts and their evaluation methods, professional quality inspectors were employed for sensory inspection. Quality defects that can be detected by touch include deformation, pits and bumps, mottling, pressure marks, pulled fibers, and wrinkling due to scratches.

Inspection method:

(1) Clean the surface of the stamped part with a clean gauze.

(2) The inspector should wear gauze gloves, close their five fingers together, and touch the surface of the stamped part along the longitudinal direction of the stamped part, feeling the unevenness of the appearance of the stamped part, and touching all surfaces and contours of the stamped part. This inspection method depends on the experience of the inspector.

(3) If necessary, the suspected area can be polished with an oil stone and verified.

Through touch inspection, it was found that four samples, Z_2, Z_3, Y_2, and Y_3, can be identified as products with qualified surface quality, while Z_1, Y_1, Y_4, and Y_5 are unqualified products.

3.2 Changes in Surface Topography of Stamping Feature Areas

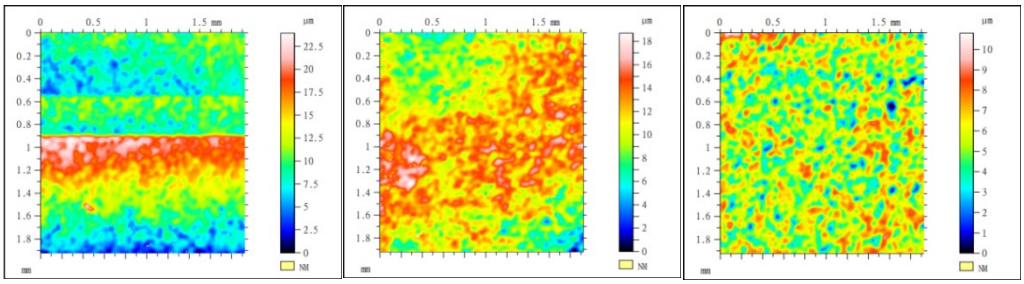

Surface of Z_1 Surface of Z_2 Surface of Z_3

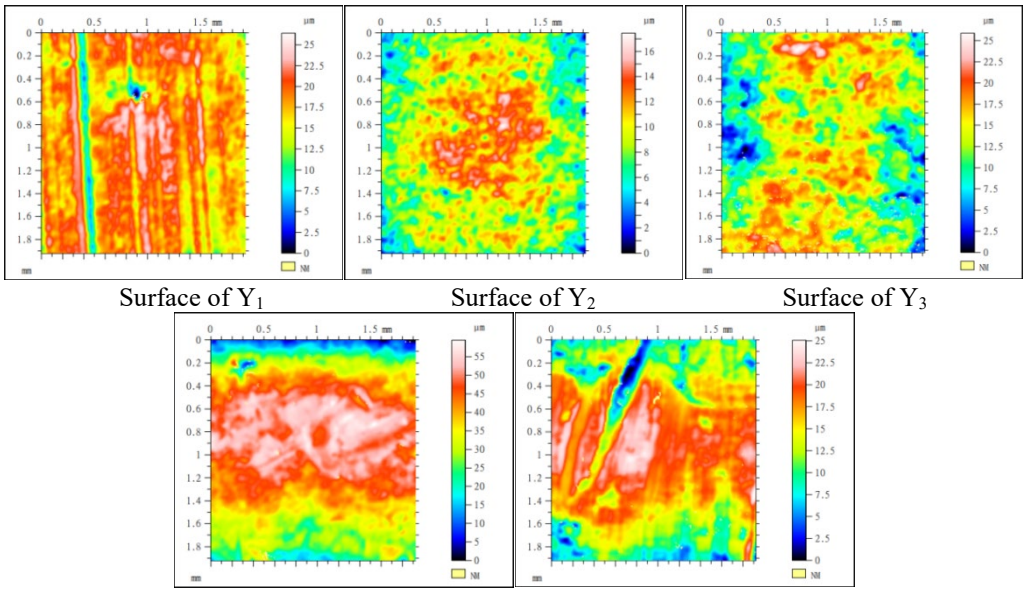

Surface of Y_1 Surface of Y_2 Surface of Y_3

Surface of Y_4 Surface of Y_5

Fig. 4. Corrected topography results of the samples

The TRIMOS TR-Scan-P 3D surface topography analyzer was used to measure the eight samples, and the corrected topography results are shown in Fig 4.

Comparing the four samples with qualified surface quality, Z_2, Z_3, Y_2, and Y_3, shown in the above figure, with the four samples with unqualified surface quality, Z1, Y_1, Y_4, and Y_5, it can be observed that:

The surface topography of qualified samples is relatively smooth, with smaller bumps and very few large peaks or valleys. On the other hand, the surface topography of unqualified samples is very rough, with larger bumps and many large peaks and valleys. Based on this, it is possible to distinguish whether the measured surface damage of the bus outer panel is qualified or not.

3.3 Preliminary determination of surface roughness threshold

The selection of threshold values for three-dimensional surface roughness is based on the analysis and comparison of measurement results from qualified and non-qualified samples. Specifically, eight samples were selected for experimental measurements, and each sample was measured three times. The three-dimensional roughness parameters were calculated for each measurement, and the arithmetic mean was taken as the final measurement result. This process yielded the maximum value of the parameters for qualified samples and the minimum value for non-qualified samples. From these maximum and minimum values, the median value was chosen as the threshold. Table 3 shows the four 3D surface roughness parameters calculated by regression Gaussian filtering.

Table 3

Calculation results of 3D surface roughness of bus outer panel

Position number	Arithmetic mean value of the same position on the samples			
	$\overline{S_q}$ (μm)	$\overline{S_{sk}}$ (μm)	$\overline{S_{ku}}$ (μm)	$\overline{S_{pd}}$ (mm^{-2})
Z_1(rejected)	4.90	0.769	5.71	55.0
Z_2(accepted)	3.36	-0.206	3.38	240
Z_3(accepted)	2.41	-0.24	3.57	246
Y_1(rejected)	3.93	0.034	4.20	147
Y_2(accepted)	3.27	-0.085	3.09	199
Y_3(accepted)	4.84	-0.188	3.09	203
Y_4(rejected)	12.9	0.215	3.91	33.3
Y_5(rejected)	5.19	0.504	3.61	167

As shown in the table, it can be inferred that the $\overline{S_q}$, $\overline{S_{sk}}$, $\overline{S_{ku}}$, and $\overline{S_{pd}}$ obtained by regression Gaussian filtering calculation can distinguish between surface quality conforming and nonconforming samples. Translation: The maximum $\overline{S_q}$ value for conforming samples is 4.84μm, while the minimum $\overline{S_q}$ value for nonconforming samples is 3.93μm. Taking the intermediate value of 4.39μm as the threshold for evaluating the conformity of automotive outer panel surface quality. The maximum $\overline{S_{sk}}$ value for conforming samples is -0.085μm, while the minimum $\overline{S_{sk}}$ value for nonconforming samples is 0.034μm. Taking the intermediate value of -0.026μm as the threshold for evaluating the conformity of automotive outer panel surface quality. The maximum $\overline{S_{ku}}$ value for conforming samples is 3.57μm, while the minimum $\overline{S_{ku}}$ value for nonconforming samples is 3.61μm. Taking the intermediate value of 3.59μm as the threshold for evaluating the conformity of automotive outer panel surface quality. The minimum $\overline{S_{pd}}$ value for conforming samples is 199mm$^{-2,}$ while the maximum $\overline{S_{pd}}$ value for nonconforming samples is 167mm^{-2}. Taking the intermediate value of 183mm^{-2} as the threshold for evaluating the conformity of automotive outer panel surface quality.

Therefore, for samples tested on site, the roughness parameters that affect surface quality are roughly calculated, and the threshold values are selected as follows: S_q = 4.39μm, S_{sk} = -0.026μm, S_{ku} = 3.59μm, S_{pd} = 183mm^{-2}.

4. Further Simulation Experiment and Quantitative Analysis

A surface roughness simulation software based on MATLAB was used for further research on whether the 3D surface roughness under the threshold parameter combination meets engineering requirements. The software uses different colors to represent the different heights of the measured points and displays the range of height data values through the color gradient of the color bar. The distribution of peaks and valleys on the measured surface is represented by different color areas.

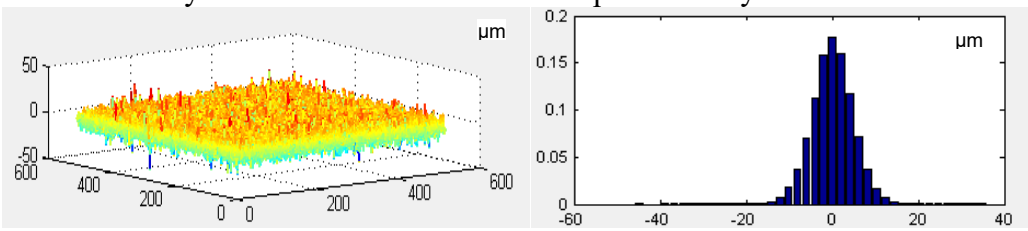

Fig. 5. Simulated surface morphology corresponding to the rough estimate parameter threshold values

Using the rough estimate parameter threshold values obtained from Section 3.3 of this article, S_q = 4.39μm, S_{sk} = -0.026μm, S_{ku} = 3.59μm, S_{pd} = 183mm^{-2} as input, the simulation software automatically analyzes and outputs the simulated 3D surface morphology. The red and yellow areas in the Fig 5 mainly describe the regions on the measured surface with large peak values and more protrusions, while the blue and green areas describe the distribution of grooves and valleys on the measured surface. It was found that there are many surface peaks, and the higher the peaks, the redder the color in the figure and the steeper the surface. From the height distribution histogram, it can be seen that the main peaks and valleys are distributed in the range of 14μm to -14μm, and the flat area accounts for 33% of the total area. It is not an ideal micro surface and is judged as nonconforming surface morphology.

In order to find more suitable threshold values for 3D roughness parameters that affect surface quality and obtain optimal surface morphology, this article conducted further simulation studies using orthogonal experimental design [22].

In light of the characteristics of the stamping formed surface described in this article, in order to obtain the optimal surface morphology, it is objective to refer to the arithmetic mean and median values of the qualified and nonconforming samples in Section 3.3 of this article when setting the experimental levels for S_q, S_{sk}, S_{ku}, and S_{pd}. Based on the above discussion, a factor-level table is constructed, as shown in Table 4.

Table 4

Factor-Level Table

Experimental levels	S_q (μm)	S_{sk} (μm)	S_{ku} (μm)	S_{pd} (mm^{-2})
1	4.39	-0.026	3.59	183

2	3.93	0.034	3.61	167
3	4.84	-0.085	3.57	199

According to the experimental factors and levels listed in Table 2, an experimental plan can be designed using the L9(3^4) orthogonal table. The numerical simulation results from the 9 experiments are then listed in the orthogonal experimental analysis Table 5 below.

Table 5

Orthogonal Experimental Analysis Table

Column	A	B	C	D	Flat Area Ratio%	Main peak-valley range
Factor	S_q	S_{sk}	S_{ku}	S_{pd}		
Test 1	A1:4.39	B1:-0.026	C1:3.59	D1:183	34	10 to -10
Test 2	A1:4.39	B2:0.034	C2:3.61	D2:167	30	15 to -12
Test 3	A1:4.39	B3:-0.085	C3:3.57	D3:199	38	10 to -10
Test 4	A2:3.93	B1:-0.026	C2:3.61	D3:199	32	11 to -11
Test 5	A2:3.93	B2:0.034	C3:3.57	D1:183	37	10 to -10
Test 6	A2:3.93	B3:-0.085	C1:3.59	D2:167	33	12 to -11
Test 7	A3:4.84	B1:-0.026	C3:3.57	D2:167	47	16 to -16
Test 8	A3:4.84	B2:0.034	C1:3.59	D3:199	31	15 to -15
Test 9	A3:4.84	B3:-0.085	C2:3.61	D1:183	28	18 to -18
Mean 1	34.000	37.667	32.667	33.000		
Mean 2	34.000	32.667	30.000	36.667		
Mean 3	35.333	33.000	40.667	33.667		
Range	1.333	5.000	10.667	3.667		

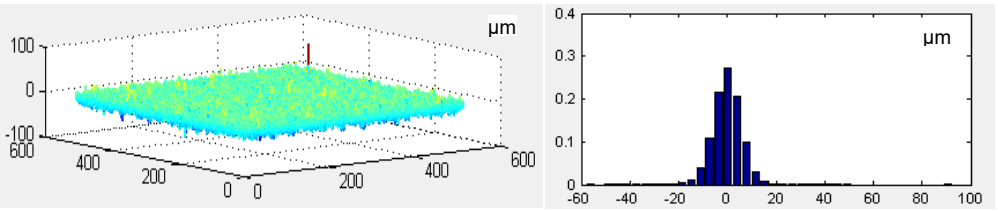

Fig. 6. Topographical morphology of the simulated surface corresponding to the optimal parameters

From the analysis of Table 4, it can be seen that the micro surface of these nine experiments obtained different levels of peak and valley shapes, with a uniform distribution of peaks and valleys and an irregular occurrence of extreme values. Through mean analysis, it can be found that the combination of surfaces such as A3, B1, C3 and D2 is the most flat, which means that the result of experiment 7. The main peak and valley are distributed in the range of 16 μm to −16 μm, accounting for 47% of the total area. As shown in Fig 6, the corresponding optimal parameters are S_q = 4.84 μm, S_{sk} = −0.026 μm, S_{ku} = 3.57 μm and S_{pd} = 167 mm^{-2}. In addition, from the analysis of the range of variation, it can be seen that among the four influencing factors, S_{ku} has the greatest influence, followed by S_{sk} and S_{pd}, while S_q has the least influence.

5. Conclusion

This study uses a 3D profilometer to obtain the surface 3D morphology of bus outer panel samples. After calculating the 3D surface roughness parameter values using regression Gaussian filtering analysis software, combined with sensory inspection by professional quality inspectors, qualified and unqualified samples are distinguished. A quantitative evaluation of surface damage on stamped parts is conducted based on the surface morphology change law. The following conclusions are drawn from the experiments: (1) Using regression 3D fast Gaussian filtering, the 3D roughness parameters Sq, Ssk, Sku, and Spd can effectively evaluate whether the surface of stamped parts is qualified. (2) Using MATLAB numerical simulation and orthogonal experiments, it can be proven that there is a clear relationship between the surface morphology features of the valve and each 3D surface roughness parameter. This indicates that using quantitative evaluation results of 3D surface roughness can to some extent distinguish the surface morphology features of stamped parts and obtain more precise threshold values, providing an efficient and accurate method for monitoring and maintaining the appearance quality of buses. (3) This research also provides a new method for quality inspection, upgrading, and transformation for bus manufacturers, improving the competitiveness and user experience of bus products. (4) The limitations of this study include a small sample size, a single material, and part shape that cannot represent the entire vehicle. Therefore, the obtained threshold values can only provide a certain reference value. However, the technical solution combining physical experiments and simulation experiments for judging surface roughness is feasible.

Acknowledgements

This article is grateful to the Project Identification of Anhui Provincial Department of Education for Promotion of Professional Services in Ten Emerging Industries (No. 2021FWXXCY017), Anhui Provincial Department of Education Natural Science Fund's key project (No. KJ2021A1178), and thanks to the experimental materials provided by Anhui BoWan Robotics Co., Ltd.

REFERENCES

[1]. *D. J.Grieve, H.Kaliszer and G. W.Rowe,* "A normal wear process examined by measurements of surface topography", in Ann. CIRP, **vol. 18**, no. 4, 1970, pp. 585-592

[2]. *C.Li and S.Dong*,"The trend of characterizing 3-D surface microtopography", in China Mechanical Engineering, **vol. 11**, no. 5, May. 2000, pp. 488-492

[3]. *K.J.Stout, P. J. Sullivan and P. A. Mckeown,* "The Use of 3-D Topographic Analysis to Determine the Microgeometric Transfer Characteristics of Textured Sheet Surfaces through Rolling", in CIRP annals, **vol. 41**, no. 1, 1992, pp. 621-624

[4]. *W.Dong, P.Sullivan and K. Stout,* "Comprehensive study of parameters for characterizing 3-D surface topography III: parameters for amplitude and some functional properties", in Wear, 1994
[5]. *H.C.Xie, D.R.Chen and X.M.Kong,* "An analysis of the three-dimensional surface topography of textured cold-rolled steel sheets",in Tribology international, **vol. 32**, no. 2 , 1999, pp.83-87
[6]. *A.Y.Suh, A.A.Polycarpou and T.F.Conry,* "Detailed surface roughness characterization of engineering surfaces undergoing tribological testing leading to scuffing", in Wear, **vol. 255**, no. 1-6 , 2003, pp.556-568.
[7]. *H.Ramasawmy and L.Blunt*, "Effect of EDM process parameters on 3D surface topography", in Journal of Materials Processing Technology, **vol. 148**, no. 2, 2004, pp. 155-164
[8]. *B.K.Li,* "Study on the law of skewness and kurtosis of three-dimensional surface", in Metrology and Measurement Technique, no. 10, 2008, pp.3-6
[9]. *N.S.Ereifej, Y.G.Oweis and G.Eliades,* "The effect of polishing technique on 3-D surface roughness and gloss of dental restorative resin composites", in Operative dentistry, **vol. 38**, no. 1, 2012, pp.E9-E20
[10]. *R.Deltombe, K.J.Kubiak and M. Bigerelle,* "How to select the most relevant 3D roughness parameters of a surface", in Scanning: The Journal of Scanning Microscopies, **vol. 36**, no. 1, 2014, pp.150-160
[11]. *R.K.Kumar, S.Seetharamu and M.Kamaraj,* "Quantitative evaluation of 3D surface roughness parameters during cavitation exposure of 16Cr–5Ni hydro turbine steel". in Wear, **vol. 320**, 2014, pp.16-24
[12]. *J.Hoła, Ł.Sadowski, J.Reiner, and S.Stach,* "Usefulness of 3D surface roughness parameters for nondestructive evaluation of pull-off adhesion of concrete layers", in Construction and Building Materials, **vol. 84**, 2015, pp.111-120
[13]. *A.Logins and T. Torims,* "The influence of high-speed milling strategies on 3D surface roughness parameters", in Procedia Engineering, **vol. 100**, 2015, pp.1253-1261
[14]. *D.Przestacki, R.Majchrowski and L.Marciniak-Podsadna,* "Experimental research of surface roughness and surface texture after laser cladding", in Applied Surface Science, **vol. 388**, 2016 , pp.420-423.
[15]. *I.Lazoglu,* "3D surface topography analysis in 5-axis ball-end milling",in CIRP Annals, **vol. 66**, no. 1, 2017, pp.133-136
[16] *S.Mordo, V.Popravko and A.Barari,* "Study of the effect of substrate on 3d surface roughness in diamond-like-carbon coating process", 2019
[17]. *V.Molnár,* "Minimization method for 3D surface roughness evaluation area", in Machines, **vol.9**, no. 9, 2021, pp.192
[18]. *W.Thasana and W.Wetchakama,* "Prediction of gloss in plastic injection parts based on 3d surface roughness from virtual machining with artificial neural networks", in International journal of automation technology, no. 2, 2022, pp.16
[19]. *Y. F.He, and H.Zhu,* "Introduction to surface quality classification and evaluation methods of foreign passenger car overlaid parts", in Automotive Technology, no. 3, 1992 , pp.56-61
[20]. *International Organization for Standardization*, "Geometrical Product Specifications (GPS) – Surface texture", in Geneva, Switzerland: International Organization for Standardization, ISO/TS 25178:2012, 2012
[21]. *W.H.Zeng, Y.S.Gao, T.B.Xie, et al,* "Fast algorithm for Gaussian filtering of three-dimensional surface roughness", in Acta Metrologica Sinica, **vol.24**, no. 1 , 2003, pp.10-13
[22]. *D. C.Montgomery,* "Design and analysis of experiments", in John Wiley & Sons, 2017